



TECHNISCHE
UNIVERSITÄT
WIEN
Vienna University of Technology



Projektarbeit

Polarization-Assisted Navigation and Water Vapor Detection Realized with MEMS

Ausgeführt am

Institut für Angewandte Physik
der technischen Universität Wien

unter der Anleitung von

Frau Prof.Dipl.-Ing.Dr.techn. Ille C. Gebeshuber

und

Herrn Univ.Prof. Mag.rer.nat. Dipl.-Ing. Dr.techn. Friedrich Aumayr

durch

Herrn Oliver Futterknecht

Wehlistraße 366/2/2

A-1020 Wien

Contents

1	Motivation	1
2	Polarization-Assisted Navigation	
	<i>Reference: [2, (Bence Suhai and Gábor Horváth, 2004)]; [8, (Wikipedia(en), 2012)]</i>	2
2.1	Polarization Vision in Humans	
	<i>Reference: [3, (Wikipedia(de), 2012)]</i>	5
2.1.1	Techniques Vikings used for Nautical Navigation	
	<i>Reference: [10, (Leif K. Karlsen, www.nordskip.com/navnotes.pdf)]</i>	6
2.2	Detectors for Polarized Skylight in Insects	
	<i>Reference: [4, (Labhart T. and Meyer E. P.)]; [5, (Labhart T. et al)]</i>	8
2.2.1	Compound eye of the honeybee	
	<i>Reference: [6, (Brines M. L. and Gould J. L., 1982)]; [7, (Valera F. G. and Witanen W., 1970)]; [11, (Rossel S. and Wehner R., 1982)]</i>	10
2.2.2	What does an insect see	
	<i>Reference: [13, (Horridge A., 2009)]; [12, (Wehner R., 1982)]</i>	13
2.3	Realisation of polarization navigation in MEMS	
	<i>Reference: [15, (Scott A.M. and Lewin A.C. and Ridley K.D., 2008)]; [17, (en.wikipedia.org, 2012)]</i>	14
2.3.1	Problems with the scattering within the atmosphere	
	<i>Reference: [17, (en.wikipedia.org, 2011)]</i>	15
2.4	A further skylight linked concept for ground navigation	
	<i>Reference: [16, de.wikipedia.org, 2012]</i>	18
2.4.1	Posibility of visualizing the wavelength of the sunbeam	
	<i>Reference: [16, de.wikipedia.org, 2012]</i>	19
3	Detection of Water Vapor	
	<i>Reference: [19, M.H. Schertenleib and H. Egli-Bronz, 2003]</i>	20
3.1	Characteristics of water vapor	
	<i>[18, Wikipedia(de), 2012]</i>	21
3.2	Methods of Cloud detection	
	<i>Reference: [20, W.B. Rossow and L. C. Garder, 1993]; [21, J. Haby, 2012]</i>	24
3.2.1	How to detect water vapor near ground	
	<i>Reference: [22, Wikipedia (en), 2012]</i>	25
4	Resume	25
	References	26
	List of Figures	28
5	Appendix	30

1 Motivation

"*Toto, I've a feeling we're not in Kansas anymore.*" [1, (Wiktionary, 2012)]. There are many occasions, when we need to find a clue where to go. Right from the beginning of humanity it was crucial to navigate from A to B, for example to get from home to the next food source. Navigation without technical devices on land was pretty easy because of defined landmarks to see where we are and where we are heading. On the sea it was harder to detect the exact position, the only clue was the position of the sun and with clear skies, the stars. But the Vikings already had some sort of compass. They were using a gemstone which changes color when the angle between the point of view and the actual position of the Sun is changing. The navigator (termed *Kendtmann* in the language of the vikings) was setting the course by gathering all the clues from the polarization, landmarks and fish- and bird migrations. So the Vikings were capable to navigate even at night, just by the informations they gathered from the Gemstone and the bearing, which the navigator gathered from the home harbor.

Nowadays we developed many different techniques and devices to improve our ability to locate our position and the destination we are heading to. For example; maps and compass or GPS navigation systems. Insects on the other side have no such equipment to get to their food sources and back home, the honeybee for example. The bee (*Apis mellifera*) is capable to find the way from and to her hive at day and nighttime. Bees are equipped with a very specialized vision; they are capable to see the pattern of polarized skylight. This ability in combination with the information from the sun and landmarks are most important for the survival of the species. Their capability is a very efficient way of navigation it is very compact and energy efficient so, for this purpose, we observe honeybees and look forward to configure MEMS that they capable to detect and analyse polarized skylight to use it as a cheap, energy efficient way to navigate just like those insects have been doing for about hundred thousand years. Furthermore it is very interesting to see if it is possible that MEMS detect and visualize small traces of water vapor near ground. There are some very interesting ways of tracking H_2O -vapor in the atmosphere and some are very easy to adapt with MEMS.

2 Polarization-Assisted Navigation

Reference: [2, (Bence Suhai and Gábor Horváth, 2004)]; [8, (Wikipedia(en), 2012)]

There are two different theories that describe the nature of light. In one light can be described as a wave and spreads as such, in the other theory light can be classified as a particle - and both theories can be proven. Combined, these theories lead to the principle of duality. For analyzing polarization the wave theory becomes our main objective. Before sunlight reaches our atmosphere it has no polarization, electric and magnetic fields are spreading in every direction. After entering the ionosphere, a defined part of the wavelength will be polarized. The greater the refraction angle, the greater is the part of the polarized light. The observed polarization pattern of the daytime sky are described by the Rayleigh sky model. The incoming light wave is reflected by air molecules, dust, aerosols and water, the resulting scattering causes the skylight to have a defined polarization pattern. These patterns are dependent on the celestial position of the sun; and at night by the reflected light of the moon. The light is highly polarized at a scattering angle of 90° from the light source. When the sun is located at the zenith the sky is polarized horizontally along the horizon. During twilight it is maximally polarized along the meridian and vertically at the horizon in the North and South, as showed in picture 1.

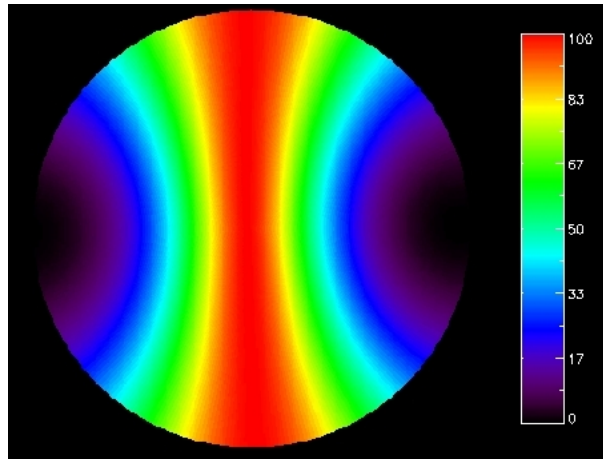


Figure 1: *This Picture indicates the degree of polarization (the Table on the right indicates the Polarization in degree) of the Rayleigh sky at sunset or sunrise.*

Ref: Halsw, <http://en.wikipedia.org/wiki/File:Degpolred.jpg>

This pattern is dependent on the position of the sun. Shown above is the pattern which appears at sunset or sunrise, where the highest polarization, vertically at the horizon, is in the North and South. The light blue band (approx. 40°) represents the circle in the North-Zenith-South plane.

The polarized patterns can be represented by a celestial triangle, based on the sun, zenith and the point of scattering, as shown in Figure 3. But the spherical triangle is not just defined by these three points but also by the interior angles as well: the three angular distances between the sun, zenith and the point defined by the observer.

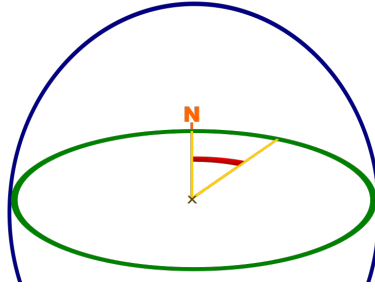


Figure 2: Simple sketch illustrating the Azimuth. green : Horizon, orange : North and red : Azimuth.

Ref: Mydriatic, vectorised by chris, <http://de.wikipedia.org/w/index.php?title=Datei:Azimuth-Simple.svg&filetimestamp=20090725154905>

In an altitude-azimuth grid (including the altitude of the sun and the azimuth, which is the angle between the observer and the natural path of the sun within the celestial sphere see Figure 2) the angular distance between the observed pointing and the sun and the angular distance between the point defined by the observer and the zenith changes while the angular distance between the sun and the zenith remains constant at one point in time. In the next Figure 4 we see the two changing angular distances as mapped onto an altitude-azimuth grid (altitude on the x-axis).

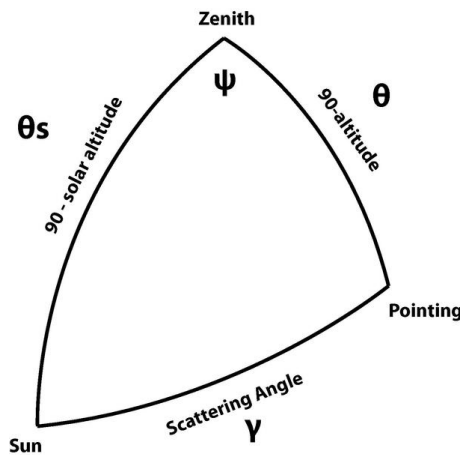


Figure 3: The geometry representing the Rayleigh sky; γ denotes the angular distance between the sun and the point of scattering, θ_s is the solar zenith distance, θ is the angular distance between the observed point and the zenith, φ is the angle between the zenith direction and the solar direction at the observed point and ψ is the angle between the solar direction and the observed pointing at the zenith.

Ref: Halsw, <http://en.wikipedia.org/w/index.php?title=File:Rayleigh-geometry.pdf> & page=1

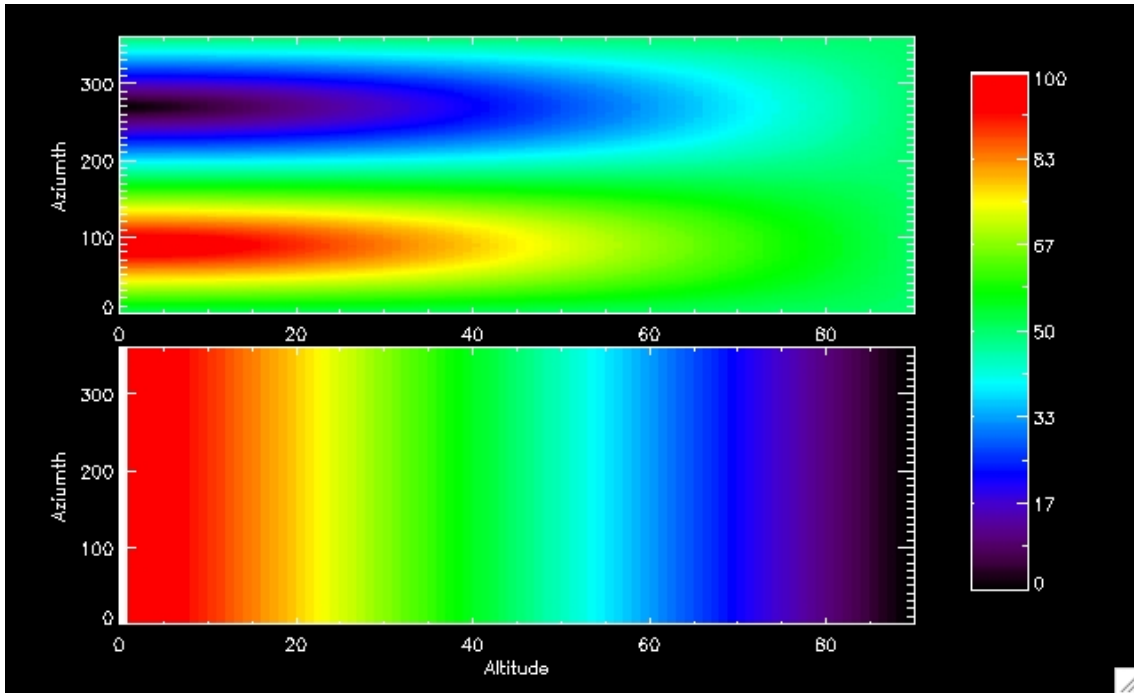


Figure 4: *The top plot shows the angular distances between the observed pointing and the sun, the bottom plot between the observed pointing and the zenith.*
Ref: Halsw, http://en.wikipedia.org/wiki/File:Soldis_zendis.jpg

We are focusing the angular distances of the triangle because those are crucial for the navigation abilities of the honeybee. There are three different models representing the different angles of the celestial triangle. There is the angle at the sun between the zenith direction and the pointing, dependent on the changing pointing and symmetrical between the Northern and Southern hemispheres (shown in the middle of figure 5), furthermore the angle at the zenith between the solar direction and the pointing which rotates around the celestial sphere (the right model in figure 5). But the most interesting is the angle at the observed pointing between the zenith direction and the solar direction: it is essential because of the dependency on the changing solar direction as the sun moves across the sky.

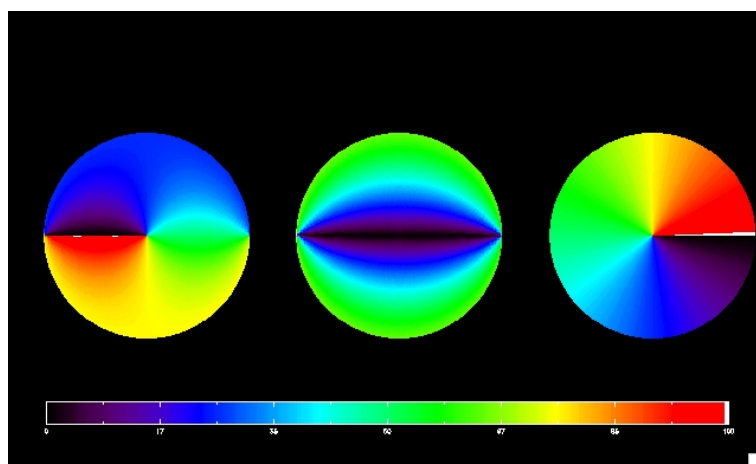


Figure 5: *The three interior angles of the celestial triangle.*
Ref: Halsw, http://en.wikipedia.org/wiki/File:Solang_ztelan_stelan.jpg

Because the pattern of polarized skylight is changing by the movement of the sun and is even reliable at twilight, it is a perfect way to navigate. The best example is the halictid bee (*Magalopta genialis*), which inhabits the rainforest's in Central America and scavenges before sunrise and after sunset. This bee leaves its nest approximately 1 hour before sunrise, forages for up to 30 minutes and accurately returns to its nest before sunrise. It acts similarly just after sunset. Thus this bee is an example of an insect that can perceive polarization patterns throughout astronomical twilight. Not only does this case exemplify the fact that polarization patterns are present during twilight, but it remains as a perfect example that when light conditions are challenging the bee orients itself based on the polarization patterns of the twilight sky.

2.1 Polarization Vision in Humans

Reference: [3, (Wikipedia(de), 2012)]

In 1844 Wilhelm Ritter von Haidinger announced in the Journal "Annalen der Physik" that humans are capable to recognize linearly and circularly polarized light. This effect is called the "Haidinger-Büschel" (see Fig. 6). So we can recognize the polarization within the wavelength of visible light, sadly the effect just arises within the eye, so it is not possible to take a picture of this effect.

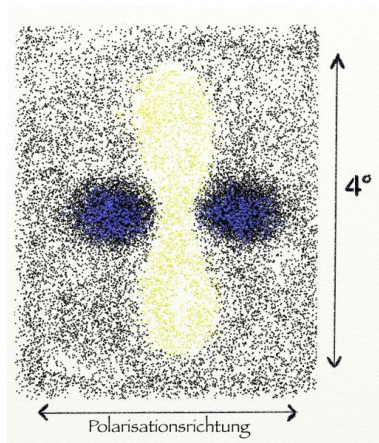


Figure 6: *Graphic of the Haidinger-Büschels (Sketch after Marcel Minnaert), the horizontal labeling says: Direction of Polarization.*

Ref: Milvus Passer, <http://de.wikipedia.org/w/index.php?title=Datei:Haidinger.klein.jpg> &filetimestamp=20090319235851

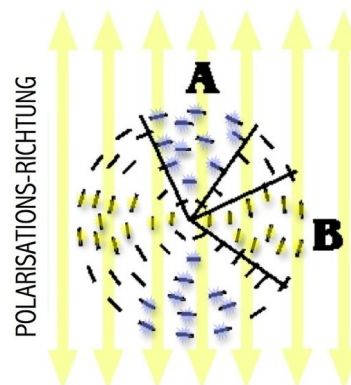


Figure 7: *Picture for explanation of the Polarization-Büschel, vertical label says: Direction of Polarization.*

Ref: Milvus Passer, <http://de.wikipedia.org/w/index.php?title=Datei:Explanation.Haidinger.jpg> &filetimestamp=20090618153508

Visualization of this effect is pretty easy, just look straight into the linear polarized light a couple of seconds and then tilt the head to the side, this effect can be reproduced by tilting the head to the other side.

When the constant polarized light beam reaches the eye it is not distinguishable from natural, not polarized light. Is the direction of the polarization changing and stays constant afterwards, so the "Polarisationbüschel" is visible for a short time and fades out like an after image. In the case of circular polarization, the "Haidinger-Büschel" is always visible. It is not fading and rotates with the polarization [3, (Wikipedia(de), 2012)].

The visualisation of the "Haidinger-Büschel" is a diffuse hourglass-shaped yellow form which is bounded in the middle by a similar blue-purple form; the form is similar to a four-leaf clover (see Figure 6). The orientation is related to the polarization direction of the incoming linear polarized light beam, its sight angle includes 3° to 4° , this implies that the expected size should be the width of two aligned Fingers, which are looked on at a stretched arm size.

To recognize the figure, the grade of the polarization of the incoming light must be at least 60% and it must include blue polarized light with wavelengths less than 500nm. The effect is much stronger with pure blue light, the yellow figure is then more of a dark blue; this might be a possible reason why the bee's ommatidia are specialized in detecting UV-light.

When the light is circular polarized, within the left and right eye the yellow part of the figure appears from the right top, to the left bottom in an angle from about $+45^\circ$. The figure is fixed to the retina and just rotates by bending the head to the side. [9, (Wikipedia, 2012)]

2.1.1 Techniques Vikings used for Nautical Navigation

Reference: [10, (Leif K. Karlsen, www.nordskip.com/navnotes.pdf)]

There are not many clues how the Vikings manage to navigate across the open ocean for thousands of miles without conventional instruments. But in many sagas are descriptions of so called sun stones and some sort of bearing board used by the Viking navigators to guide them across the North Atlantic. The Vikings mostly sailed in summer, this habits support the theory, because then the Northern latitudes are experiencing long days and short nights. So the Vikings where depending more on the sun than to the stars for navigation.

So it was common to use a crystal which is able to even change color by the angle the sunbeam is entering the crystal for example a Corderit (see the color changing over time in the Appendix) or a crystal which is known for its double refraction like the Icelandic spar. For the last form of navigation, it is crucial that the sun itself is visible, so that the sunbeam hits the device directly. While the first sort of crystal needs only the polarization of the sunbeam which leads to the change of colors even when the sun is not directly visible and even at night, when the moon is reflecting the rays coming from sun.

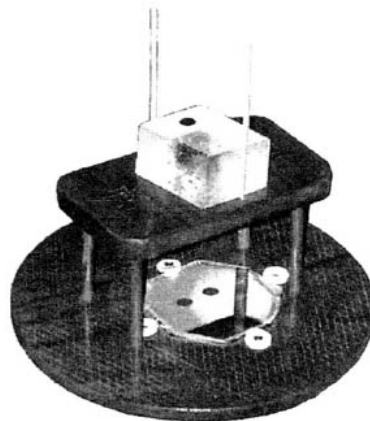


Figure 8: Sunstone stand of build by Leif K. Karlsen, showing the black dot on top of an Iceland spar and the reflected double dots in the mirror underneath.

Ref: Leif K. Karlsen, Viking Navigation Using the sunstone, Polarized light and the Horizon board, in: Navigation Notes, Issue 93, pp 5-8, <http://www.nordskip.com/navnotes.pdf>

2.2 Detectors for Polarized Skylight in Insects

Reference: [4, (Labhart T. and Meyer E. P.)]; [5, (Labhart T. et al)]

Apart from the sun, the polarization pattern of the sky offers insects a reference for visual compass orientation. The detection of the oscillation plane of polarized skylight is mediated exclusively by a group of specialized ommatidia (which are the small units build up the compound eye, see Figure 10) situated at the dorsal rim area of the compound eye (DRA, dorsal rim area, see Figure 11).

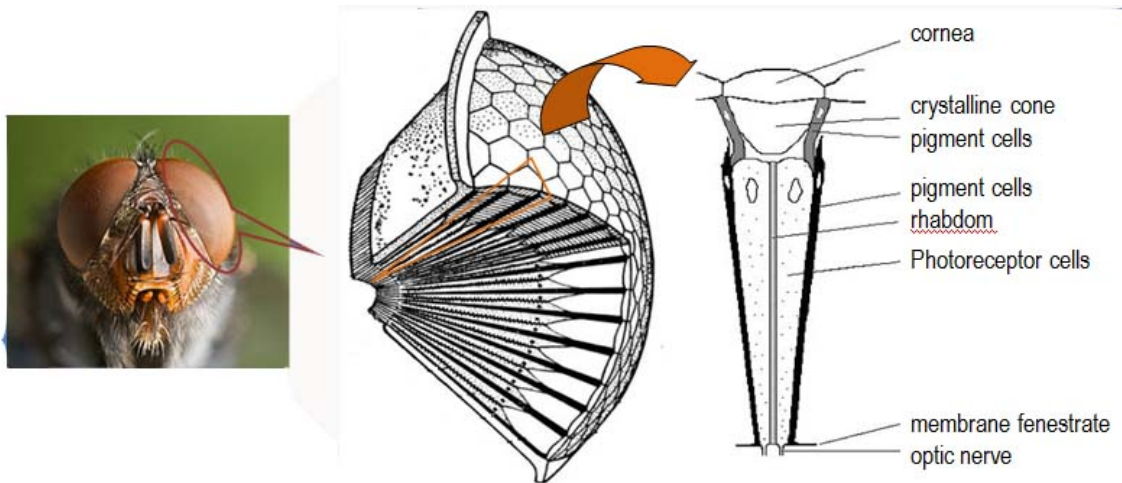


Figure 10: Picture of the compound eye of the honeybee, defining the ommatidia.
 Ref: [en.wikipedia.org](http://en.wikipedia.org/wiki/Compound_eye#Compound_eyes), http://en.wikipedia.org/wiki/Compound_eye#Compound_eyes

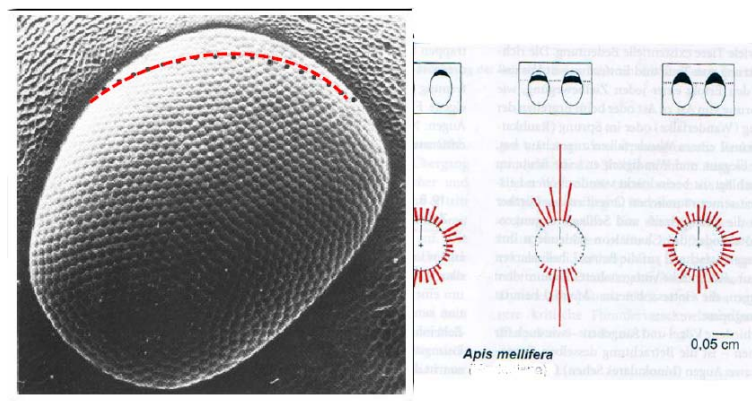


Figure 11: DRA (delineated by the red line) of the honeybee.
 Ref: Penzlin H.: *Lehrbuch der Tierphysiologie*, Vers. 7, München: Spektrum Akademischer Verlag, 2005, pp 781–784

The physiological specification of the DRA goes along with characteristic changes in ommatidial structure, providing actual anatomical hallmarks of polarized skylight detection, that are readily detectable in histological sections of compound eyes. The presence of anatomically specialized dorsal rim ommatidia in many other insect species belonging to a wide range of different orders indicates that polarized skylight detection is a common visual function in insects.

The key function of the DRA of the compound eye for E-vector perception has been demonstrated in four insect species by behavioral experiments (for example in the honeybee, *Apis mellifera*: Wehner and Strasser, 1985). As shown by electrophysiological recordings, the dorsal rim ommatidia of this species share a number of physiological properties that makes them especially suitable for the detection of polarized skylight: each ommatidium contains two sets

of homochromatic, strongly polarization-sensitive photoreceptors with orthogonally arranged analyzer directions.

As revealed in the honey bee, which has nine instead of eight long receptor cells, it is the three UV-receptors R1,5,9 (see Figure 13) that mediate polarization vision in the bee, forming large rhabdomeres (light-conducting axle rods) with orthogonal microvillar orientations (microvilli are thin threadlike cell processes used to maximize the surface, see Figure 14). In addition, the DRA of *Apis* has straight retinulae as opposed to the regular retinulae that are twisted about their long axis. This allows a higher absorption of the UV-waves because the ray can enter the ommatidium without reflections within the retinulae. So in honey bees the strict alignment of the microvilli along the rhabdom was shown to boost polarization sensitivity of the UV-receptors [4, (Labhart T. and Meyer E. P.)].

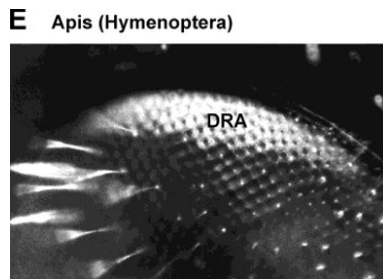


Figure 12: *Honey bee Apis mellifera* (Hymenoptera): The dorsalmost eye part of an intact eye as seen with incident illumination reveals light-scattering pore canals in the cornea of the DRA.

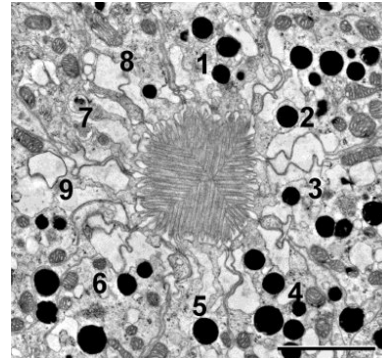


Figure 13: *Electron micrograph of the dorsal rim retinulae situated within an ommatidium. It contains nine (instead of eight like locust DRA) long receptor cells, the UV-cells of which have their microvilli oriented strictly orthogonal to each other. (Scale bar 2 μ m)*

Ref: T. Lambhart and E.P. Meyer, Detectors for Polarized Skylight in Insects: A Survey of Ommatidial Specializations in the Dorsal Rim Area of the Compound Eye, in: Microscopy Research and Technique, Vol. 47, p 372, 1999

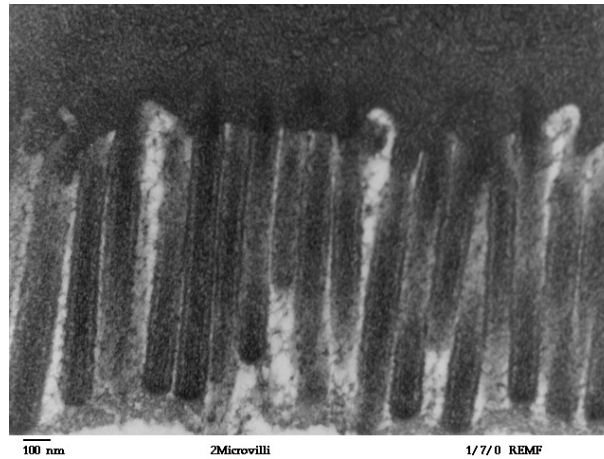


Figure 14: Transmission electron microscope image of a thin section cut through a human jejunum (segment of small intestine) epithelial cell. This high magnification image of MV1 Image shows some of the densely packed microvilli that make up the striated border. Each microvillus is approximately 1 μm long by 0.1 μm in diameter and contains a core of actin microfilaments. Ref: L. Howard and K. Connolly, http://en.wikipedia.org/wiki/File:Human_jejunum_microvilli_2_-_TEM.jpg

2.2.1 Compound eye of the honeybee

Reference: [6, (Brines M. L. and Gould J. L., 1982)]; [7, (Valera F. G. and Witanen W., 1970)]; [11, (Rossel S. and Wehner R., 1982)]

Now for many invertebrate animals are these patterns crucial to determinate their position, because when the sun is hidden behind clouds, trees or the horizon they rely on the information provided by the patterns of polarized skylight. The interesting fact is, that the E-vector patterns correspond more closely to predictions based on first order (Rayleigh), scattering at 650 nm and 500 nm than to 350 nm (UV). Most insects, including the honeybee, respond to polarization patterns only at UV wavelengths which seems to be inefficient but on the other hand the quality of those patterns is increasing when the sun is hidden behind clouds, trees or the horizon. Under those special and difficult conditions ultraviolet light has advantages over longer wavelengths, because the resulting reflections present more troublesome interference at longer wavelengths than in the UV [6, (Brines M. L. and Gould J. L., 1982)].

The compound eye of the honeybee is a very complex system which is capable to perceive UV-light and analyze the polarized skylight pattern. It is made up of very small units called ommatidia, each ommatidium (see Fig. 16) contains an optical system and seven to eight receptor cells. In the insects, rhabdomeres from several retinula cells may fuse to form a central, closed rhabdom; but in certain bee's eyes there is no fusion, and the rhabdomeres remain isolated from one another and this spatial isolation permits each retinula cell to act as an individual receptor [7, (Valera F. G. and Witanen W., 1970)]. The following graphic (see Fig. 15) shows a cut view of a compound eye.

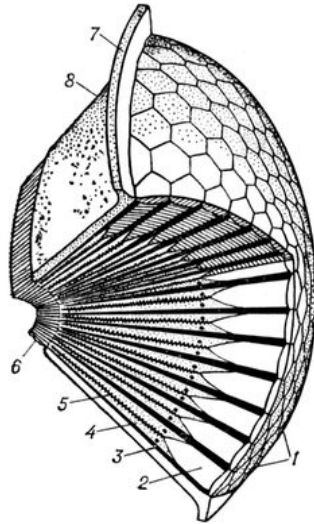


Figure 15: *Anatomy of the compound eye of an insect.*
 Ref: *Great Soviet Encyclopedia*, [http://en.wikipedia.org/wiki/
 File:Compound_eye1.jpg](http://en.wikipedia.org/wiki/File:Compound_eye1.jpg)

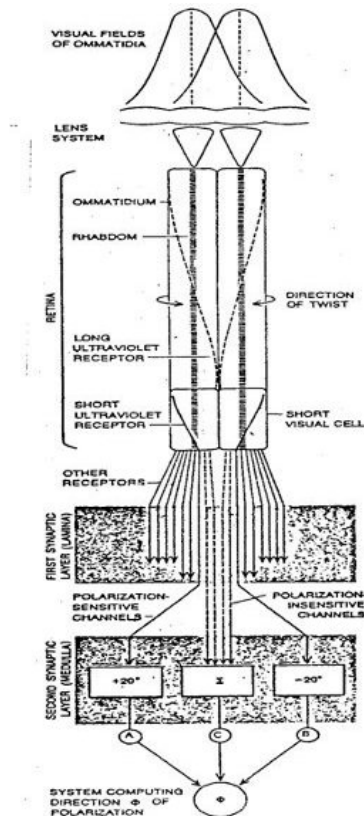


Figure 16: *Model of a honeybee's ommatidium.*
 Ref: *B. Schricker and B. Polaczek, Seminar:Biologie der Bienen, Author: Marco Block*

There are many studies about the orientation of the honeybee showing the ability of the bee to navigate. Using a horizontally arranged hive containing a single comb. The hive can be moved in the x and y directions, covered by a Plexiglas hemisphere equipped with coverable windows through which when they are opened, either natural sky light or artificially polarized light can be presented to the bees. For the artificial light source a Xenon arc with heat filters, diffusers, spectral light filters and polarizers are used. Also a TV camera, monitor and video recorder are installed. With this installation [11, (Rossel S. and Wehner R., 1982)] Russel and Wehner

discovered, that honeybees should be able to orient correctly whenever they can view at least two E-vectors in the sky (two E-vectors are necessary when identical directions of polarization occur twice at the elevation concerned) However, even under such apparently unambiguous stimulus conditions, bees make mistakes. This holds true even if they have had the chance to view the full E-vector as it occurs in the sky and thus cannot rely on memorized images of the E-vector patterns so what they seem to use instead is a celestial map that provides not a correct but an approximative compass information about the actual E-vector patterns in the sky.

2.2.2 What does an insect see

Reference: [13, (Horridge A., 2009)]; [12, (Wehner R., 1982)]

The eye of *Apis mellifera* is an array of photo receptors, each at an angle to the next, so its perception is just like the human eye, except that it is not inverted. The architecture of the eye tells us a little about what the bee actually abstracts from the panorama. It is also not sufficient to determine whether bees recognize patterns or just gather a series of cues to navigate to the target.

Below the photo receptors, the next components of the sensory mechanism are small feature detectors that are one, two or three ommatidia wide that respond to light intensity, direction of passing edges or orientation of edges displayed by parameters in a pattern. At the next stage responses of the feature detectors for area and edges are summed in various ways in each local region of the eye to form several types of local internal feature totals, here called cues. Cues representing the units of visual memory in the bee, at next stage summation implies that there is one of each type in each local eye region and that local details of the pattern are lost [13, (Horridge A., 2009)].

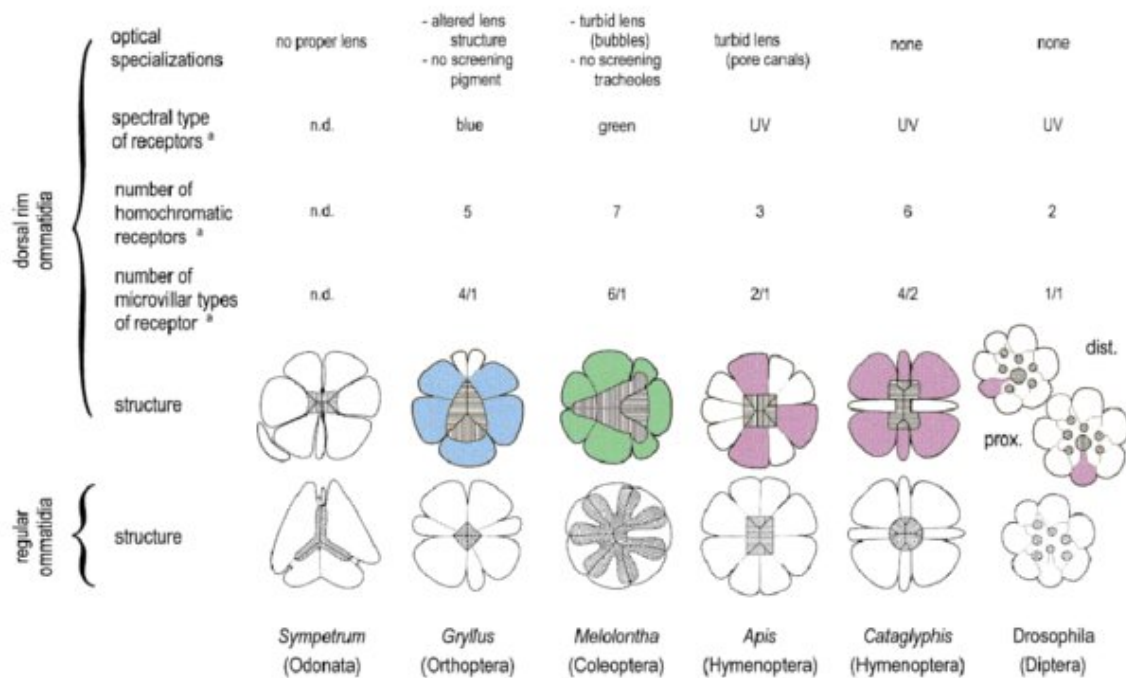


Figure 17: Comparison between optical, spectral and structural details of the specialized ommatidia in the dorsal rim area of different insects. Colors indicate spectral receptor type; violet stands for UV. ^aSpectral type of receptor that mediates polarization vision, not counting a possible small, proximal receptor.

Ref: T. Lambhart and E.P. Meyer, *Detectors for Polarized Skylight in Insects: A Survey of Ommatidial Specializations in the Dorsal Rim Area of the Compound Eye*, in: *Microscopy Research and Technique*, Vol. 47, p 372, 1999

So insects have developed many different forms of analyzing the polarized skylight for clues to determine their traveling vector. To get a closer look on how the honeybee uses the E-vector for their navigation from the hive to their food sources and back, lets recapitulate the main tools empowering such a great ability. The E-vector pattern in the sky can be described most conveniently by a sun-related system of coordinates determined by the Rayleigh Sky model described above. On how the honeybee uses this information can be extrapolated from the hypothesis, that bees are supposed to memorize the E-vector pattern last seen, and later match the current image (i.e. the actual pattern when they fly back) with the memorized one. Therefore

bees should be able to orient correctly whenever they can view at least two E-vectors in the sky (two E-vectors are crucial when identical directions of polarization occur twice at the elevation they orient on [12, (Wehner R., 1982)]). But there is still one problem to fully understand on how bees really using E-vector informations. Rossel and Wehner research showed that bees (even when they see the full E-vector pattern) still make navigation mistakes, so it seems that they are using not directly the information given by the E-vector. Instead they build up some sort of celestial map providing approximative compass information about the actual E-vector patterns [11, (Rossel S. and Wehner R., 1982)]. With this information the honeybee can approximate the way from and back their hive including the information from the inner celestial map and landmarks they memorize before they flew of.

The next step is to discuss how to apply this ability to a small, energy efficient device.

2.3 Realisation of polarization navigation in MEMS

Reference: [15, (Scott A.M. and Lewin A.C. and Ridley K.D., 2008)]; [17, (en.wikipedia.org, 2012)]

A polarization-based navigation device can be realized by using the geometrical connection between the three points of the Rayleigh sky model [see Figure 3], using an optical angle detection MEM. The apparatus found fitting for this purpose is a light angle detector MEM. It is already patented in the US and mainly consists of two optical detectors, the first is placed in front of a coating or layer with optical transmission ability, this layer transports the beam to the second detector, the refraction developed by the coating defines the characteristic of the measured data [see Figure 19]. The difference in the light characteristics measured at the respective detectors therefore provides an indication of the angle of incidence of the light beam. [15, (Scott A.M. and Lewin A.C. and Ridley K.D., 2008)]

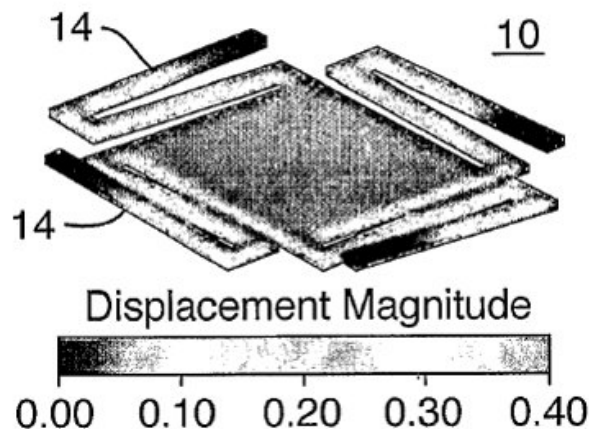


Figure 18: *A perspective view of a typical micromirror element and typical spring structures of the angle detection MEMS. (10) micromirror, (14) springs. Copiright holder [15, (Scott A. M. and Lewin A.C. and Ridley K. D., 2008)].*

Ref: A.M. Scott and A.C. Lewin and K.D. Ridley United States Patent Application Publication, in: US Patent Application, Pub.No.: US 2008/0266553A1, 30. Oct.2008

Using this MEMS and apply the law of cosines to the spherical triangle it gives:

$$\cos(\gamma) = \sin(\theta_s)\sin(\theta)\cos(\psi) + \cos(\theta_s)\cos(\theta) \quad (1)$$

This equation is used to calculate the scattering angle between the observed pointing and the sun. For θ_s is the solar zenith distance (90° - solar altitude), ψ is the angle between the solar direction and the observed pointing at the zenith, θ is the angular distance between the observed pointing and the zenith (90° - observed altitude) and γ is the angular distance between the observed pointing and the sun.

This equation reaches a singularity at the zenith where the angular distance between the observed pointing and the zenith θ_s , is zero. Here the orientation of polarization is defined as the difference in azimuth between the observed pointing and the solar azimuth. The scattering plane is the plane through the sun, the observer, and the point observed (or the scattering point). The angle ψ located at the zenith between the solar direction and the observed pointing is the scattering angle. This angle of polarization is always perpendicular to the scattering plane. [17, (en.wikipedia. org, 2012)]

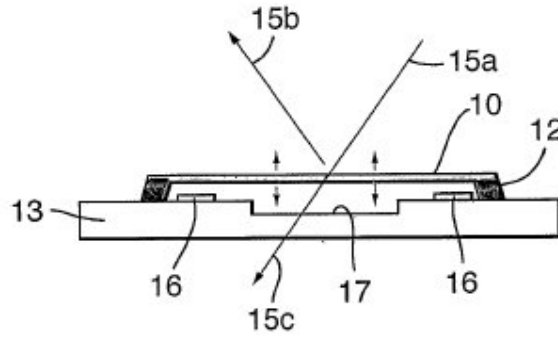


Figure 19: Shows a side view of the micromirror element and typical spring structures. (10) micromirror, (12) suspension, (13) substrate, (15a, b, c) light path, (16) bushes(isolated islands), (17) dimple. [15, (Scott A. M. and Lewin A. C. and Ridley K. D., 2008)].

Ref: A.M. Scott and A.C. Lewin and K.D. Ridley, United States Patent Application Publication, in: US Patent Application, Pub.No.: US 2008/0266553A1, 30. Oct.2008

With this information it is possible to calculate the angle dependent grade of polarization:

$$\delta_{polarization} = \frac{I_{\parallel} - I_{\perp}}{I_{\parallel} + I_{\perp}} \Rightarrow \frac{1 - \cos^2(\alpha)}{1 + \cos^2(\alpha)} \quad (2)$$

It is correlated to the angle $\alpha = 90^\circ - \theta$ which is the angle between the observed pointing and the sun. Therefore we could use the same clues as the honeybee, to provide enough information for ground navigation.

2.3.1 Problems with the scattering within the atmosphere

Reference: [17, (en.wikipedia.org,2011)]

One major technical problem is still unsolved: the sunlight has to go through different layers of our atmosphere, where Rayleigh scattering takes place [17, (en.wikipedia.org,2011)] and from which we get the pattern for our navigation. However, when near strong reflecting surfaces such as water or ice, the reflection of the ground is stronger than the one from the polarized sky pattern. Therefore we have the problem that the first reflection from the sky is overpowered by the one from ground and the MEMS could have troubles differating them.

One solution could be to turn the angle of the MEM, so that it has a 45° angle in comparative to the ground. So we can exclude most of the sources coming not from the skylight pattern. In nature there are many different solutions for this problem. First of all is in every compound eye mainly the Dorsal rim area (DRA) the main sensor array for detecting the skylight polarization. It is situated in the upper third of the compound eye and therefor always orientated to the sky (see Figure 11). The Harlequin beetle for example has its Dorsal rim area (see Chapter 2.2 *Detectors for Polarized Skylight in Insects*, page 9) mechanical separated above its antennas (see Figure 20).....



Figure 20: The head of a Harlequin beetle.
 Ref: Photograph and Copyright by Iwan Ramawan.
<http://500px.com/photo/3277004>



Figure 21: Picture of a Harlequin beetle (*Acrocinus longimanus*).
 Ref: Werner Rose. Original uploader Bupresits at de.wikipedia,http://de.wikipedia.org/w/index.php?title=Datei:Acrocinus_longimanus.jpg&filetimestamp=20101024_111847

Furthermore the device is detecting all light waves, that means the strongest source will be the first to notice. Now artificial sources of light can also irritate the device, which makes it not usable within public areas, where the light pollution is increasing. Bees have the same problem in public areas with light pollution, but they are able to divert the natural from the artificial light waves. Additionally the European bee (*apis mellifera*) is only active when the sun is shining. So the strongest light comes from the sun, when the bees are flying out. They are not flying when the weather is dizzy or it is raining (when the artificial lighting is the strongest source).

In the tropics on the other hand, the central American bee (*megalopta genalis* see Figure 22) is only active at night. Until now we just know that these bees also using landmarks to find their way back to the hive but their eyes are just 30 times more photosensitive than the eyes of the European bee. So it is not completely clear if *megalopta genalis* is more distracted from artificial light than *apis mellifera*.



Figure 22: Head of the central American bee (*megalopta genalis*).
 Ref: University Lund, <http://www.g-o.de/wissen-aktuell-1356-2004-08-11.html>

It is not just simply the pollution which could produce wrong readings. There is also one fact that counts. The sun is emitting electromagnetic radiation from 250 nm to 2500 nm (see Figure 23).

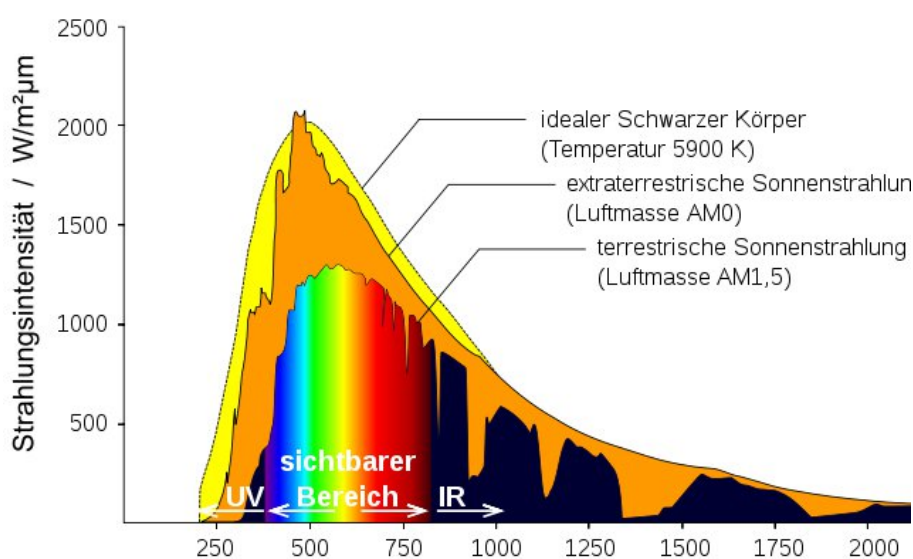


Figure 23: Sun radiation above and on the earth's surface. The abscissa is showing the wavelength and the ordinate the intensity of the radiation. Where the yellow curve is the ideal black radiator at 5900°K, the orange curve represents the extraterrestrial sun radiation with the Airmass AM0, and the colored, black curve is the terrestrial sun radiation with the Airmass AM1.5.

Ref: Degreen at [de.wikipedia](http://de.wikipedia.org), later Quilbert at [de.wikipedia](http://de.wikipedia.org), http://de.wikipedia.org/w/index.php?title=Datei:Sonne_Strahlungsintensitaet.svg&filetimestamp=20100509_202305

The visible bandwidth (for humans) is in the area of 380 nm to 780 nm. There the scattering effect within the atmosphere is the strongest, which gives a perfect basis to generate the polarized pattern within open areas, but in nature for example in forests or at night, there the visible light scattering is causing great disturbances that causes deviations in the device. Here the UV spectrum is the wavelength area of choice. The shorter the wavelength of the UV (around 250 nm to 280 nm) the lesser the scattering within the atmosphere and the clearer the cue to the polarization pattern in the sky.

This problem should be easily solved by mounting a UV-Filter or using a fitting coating layer between the two light detecting surfaces of the MEMS.

2.4 A further skylight linked concept for ground navigation

Reference: [16, de.wikipedia.org, 2012]

The polarization pattern in the sky is not the only way to provide data for ground navigation. There is also the wavelength of the lightwave emitted by the sun and also the measurement of the earths magnetic field. Where at dusk and dawn the sky appears to be red (see Figure 24), during the day the sky is blue this effect is also usable for ground navigation.

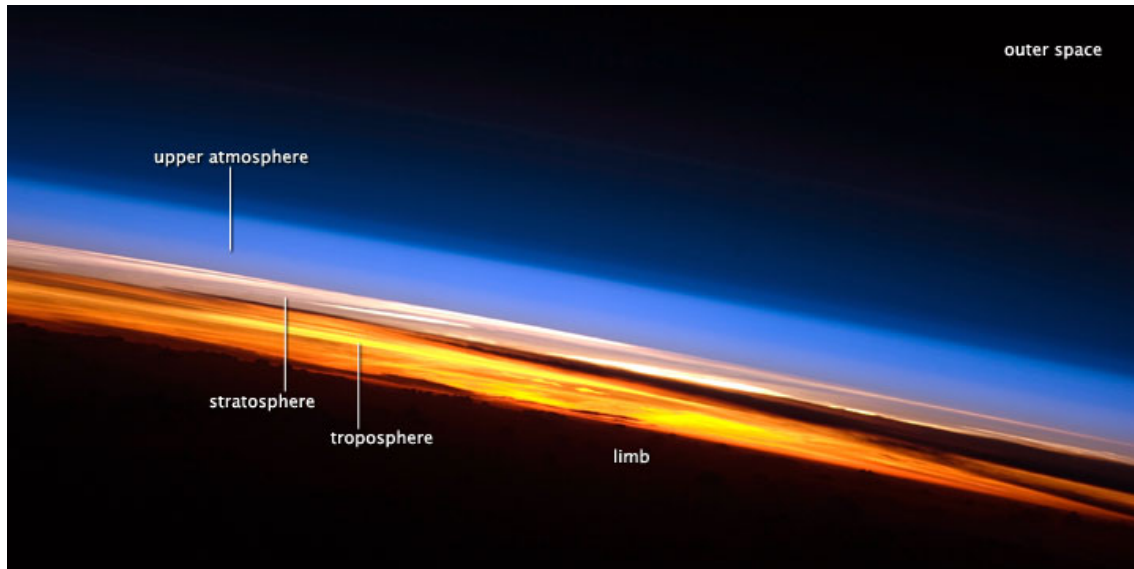


Figure 24: *Limb view of the Earth's atmosphere. Colors roughly denote the layers of the atmosphere.*

Ref: NASA Earth Observatory, <http://earthobservatory.nasa.gov/IOTD/view.php?id=44267>

By the clue, delivered from the sun, we can calculate the approximate distance from the zenith regarding the azimuth and the altitude of the sun. This is enough to determinate the position relative to the sun. Because this is not enough information to calculate position on the ground, we need to apply some different methods to rise the accuracy of this technique. But in combination with the polarized skylight orientation, this method could provide additional information and with it the possibility to navigate just relying on the sky. One of them, described in the next chapter, we are using the distance of the sun from earths surface to calculate the distance of the spectators point from the equator (see Figure 25).

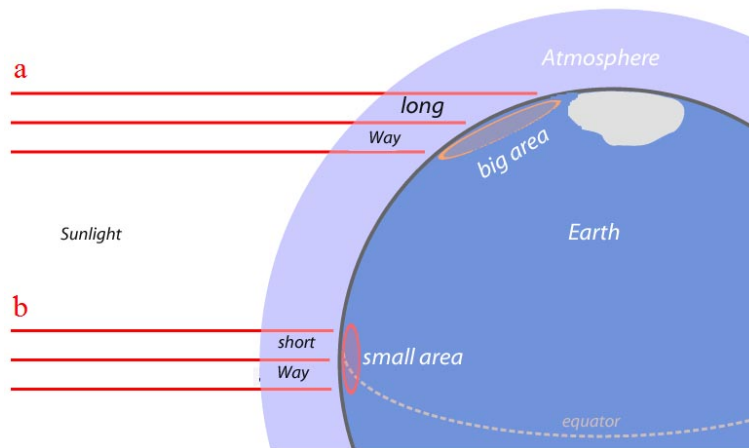


Figure 25: Schematic sketch of the different intensity and distances the sunlight has to cover, resulting in different wavelengths, resulting in different visible colors. a: long way, reaching an impact angle around 65° creating approximate 700 Watt/m^2 . b: short way, reaching an impact angle around 90° creating approximate 970 Watt/m^2 .

Ref: Cepheiden, http://de.wikipedia.org/w/index.php?title=Datei:Oblique_rays_04_Pengo_DE.svg&filetimestamp=20110223080939

2.4.1 Possibility of visualizing the wavelength of the sunbeam

Reference: [16, de.wikipedia.org, 2012]

There is the possibility to use a luxmeter to measure the intensity of the incoming sunbeam to determine the approximate position from the viewer to the equator, but the huge problem is, that the light beam is scattered within the atmosphere, so that the readings are not accurate enough.

Also the use of a luxmeter is a non accurate option, because the intensity of the sunlight is depending on so many factors, that the result is no exact clue to calculate the position relative to the sun.

An alternative could be a Pyranometer (see Figure 26) which measures the incoming global sun radiation. Afterwards analyzing the intensity for peaks which are typical for the distance the sun has at specified points at the sky. Thereby it would be possible to verify and improve the Data received by the Light angle detection MEMS. Because of the increasing processing power needed for analyzing the additional Data it is not sure if it is an improvement to install this additional device.



Figure 26: Picture of SR11 Pyranometer to measure the radiation flux density of the sun.

Ref: Hukseflux2008, http://de.wikipedia.org/w/index.php?title=Datei:Pyranometer_sr11_hukseflux.gif&filetimestamp=20080805101001

3 Detection of Water Vapor

Reference: [19, M.H. Schertenleib and H. Egli-Bronz, 2003]

Meteorology goes back to the time of Aristoteles, where every form appearing in the sky was a meteor (Greek, for floating in the air. Aristoteles described weather phenomena like clouds, rain, etc.), which were unpredictable and not directly calculable from the laws of nature known then. The more far away stars were seen predictable and the main task for astronomy, the border for them was the moon. With time, weather became a little bit more predictable and forecasts where made by observation of the weather and keeping track of the changes.

Nowadays we keep track of clouds by using data from various sources, for example weather balloons, satellites or radar facilities(see Figure 27). Accumulation of the data and calculating with floating formalism we obtain a forecast that is up to 65% accurate.

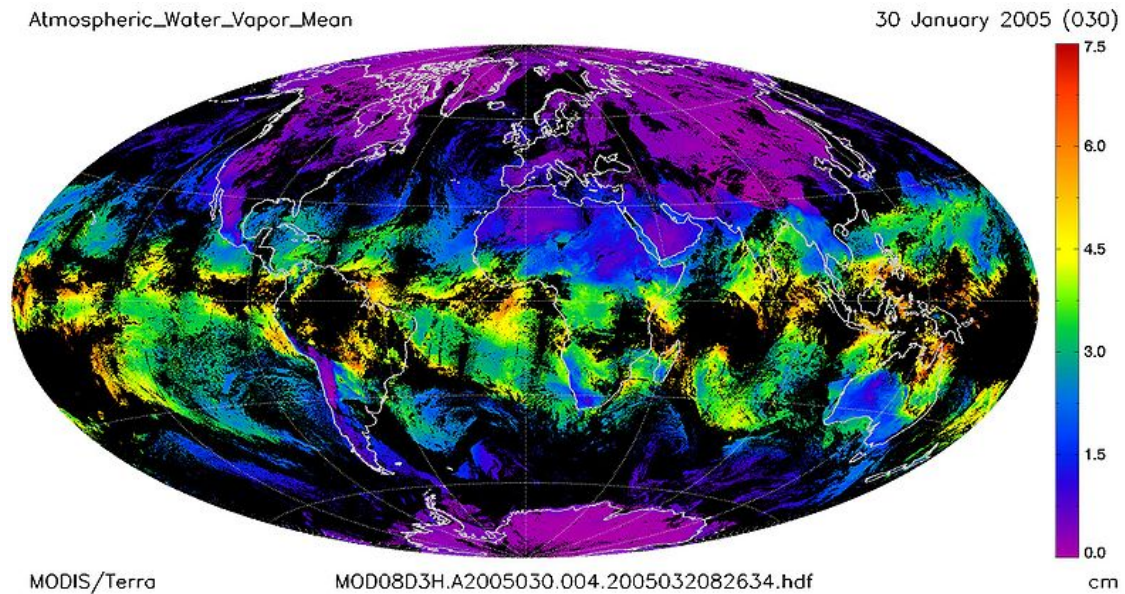


Figure 27: Allocation of the water vapor in the Earth's atmosphere. The condensated water vapor within an air column over one square meter is denoted in centimeters.

Ref: Saperaud, http://de.wikipedia.org/w/index.php?title=Datei:Atmospheric_Water_Vapor_Mean_2005.030.jpg&filetimestamp=200507_30141431

This techniques, using radar to actually detect water vapor in the atmosphere could be used to detect water near ground. To be exactly the water vapor which leaves the soil layers. This could be used to trace water in the desert, finding the course of a dried out river and preventing adventurers from dying of thirst. Also there could be a possibility to detect the ideal place to dig a well.

3.1 Characteristics of water vapor

[18, Wikipedia(de), 2012]

At about 1.013 bar water is boiling at 100 °C; is the water still heated, there will be no more raising in temperature, instead the water will be vaporizing. One liter water becomes 1673 litres of water vapor which takes about 2.257 kJ (see Figure 28).

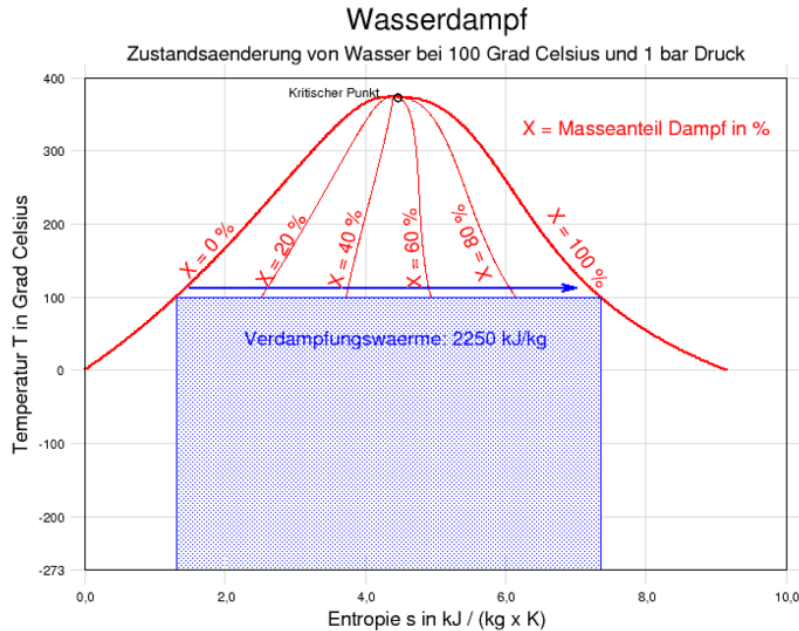


Figure 28: *T-S-Diagram of water vapor at 100 °C, the ordinate says: Temperature T in °C and the abscissa says: Entropy s in kJ / (kg x K) which is actually the specific entropy of water vapor.*

Ref: Markus Schweiß, http://de.wikipedia.org/w/index.php?title=Datei:TSWasserdampf_100.png&filetimestamp=20051217215345

The vapor pressure of water is depending on the temperature; within temperatures below the boiling point it is defined as evaporation.

We can differentiate between:

Wet Vapor: when vapor emerges in colder areas emerge and a part of the vapor condense to fine drops. The mass of the wet vapor within fluid water is calculated with the following formula:

$$x = \frac{m_{Vapor}}{m_{Fluid} + m_{Vapor}} \quad (3)$$

Hot Vapor: which is divided in two forms:

1. Overheated steam, which is vapor, hotter then the boiling temperature. The steam is dry and does not consists of drops. This form of damp is created in steam boilers.
2. Overcritical damp, atop the critical point(see Figure 28), water vapor and water fluid are no longer discriminable regarding their density.

Saturated Vapor or Dry Saturated Vapor exists at the border between wet- and hot vapor and most tabular values of water vapor states refer to this point.

The gas form of water or overheated damp is without color and firmly invisible. Wet vapor on the other side is visible, because of the carried away drops. Water vapor can be retrieved directly from its massive state (ice), this phenomenon is called, sublimation.

The Mollier-Diagram shows the entropy of vapor at the abscissa and the corresponding enthalpy on the ordinate. The change in state of the vapor with its needed heat can be seen directly on the ordinate (see Figure 29).

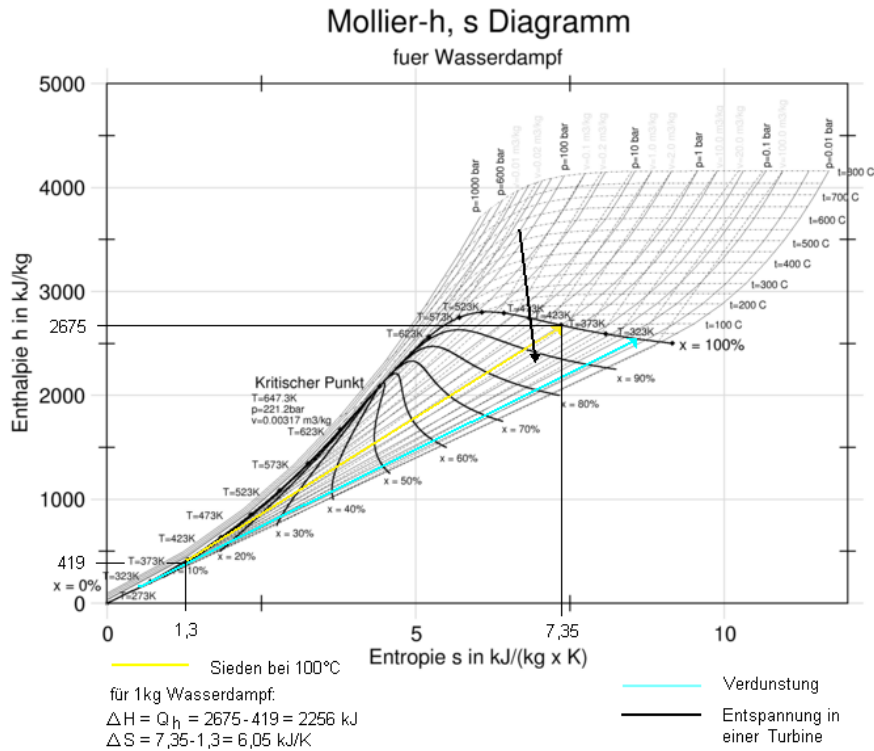


Figure 29: Mollier-h, s diagram for water vapor. The x-Axis named Entropie in kJ/(kg * K) is actually the specific Entropy for Water Vapor.

Ref: Markus Schweiß, http://de.wikipedia.org/w/index.php?title=Datei:HS_Wasserdampf_SW.png&filetimestamp=20051207070514

The saturation of water vapor in the air is also depending on the temperature (see Figure 30).

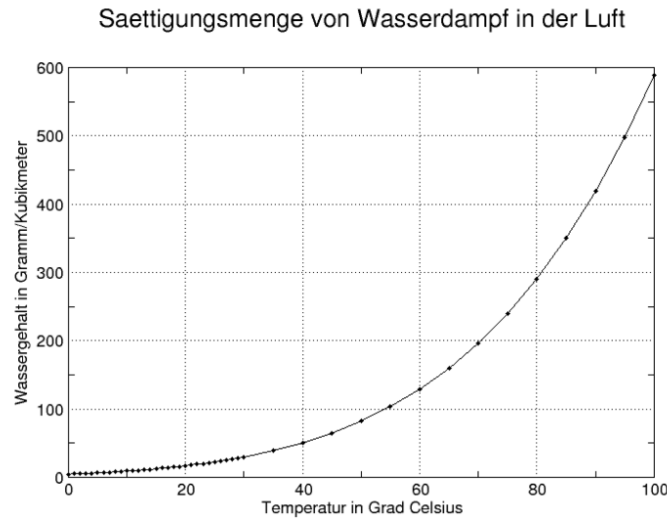


Figure 30: *Saturation of water vapor within the air, the ordinate says: Water mass in gram per cubic meter and the abscissa says: Temperature in degree Centigrade.*

Ref: Markus Schweiß, http://de.wikipedia.org/w/index.php?title=Datei:Feuchte_Luft.png &filetimestamp=20051120170646

Generally one kilogram air at 30°C and one bar pressure can hold about 26 grams of humidity. This amount falls at 10°C to about 7.5 g/kg, the overflow is, depending on the weather, released as rain, snow, hail or fog. The clouds act as reflecting layer for most of the sunlight reaching the Earth. The water vapor within the atmosphere is from 36% up to 70%. It is the main source of the counter radiation off the Earth's surface and trigger of the natural greenhouse effect [19, Globale Klimatologie: Meteorologie, Wetterinformation und Klimatologie].

3.2 Methods of Cloud detection

Reference: [20, W.B. Rossow and L. C. Garder, 1993]; [21, J. Haby, 2012]

Currently there are two ways to keep track of clouds, firstly, the visible satellite imagery (VIS) (see Figure 31) and the second the infrared imagery (IR) (see Figure 32). Where the visible imagery is produced by the sun's rays reflection off of clouds. IR images are produced by sensing the emitted radiation coming off clouds. The temperature of the cloud will determine the wavelength of radiation emitted from the cloud.

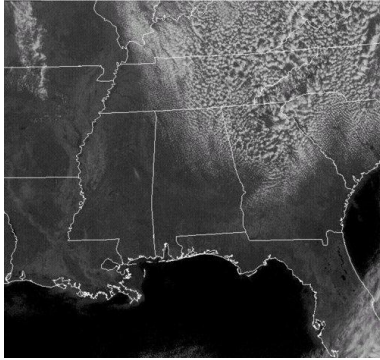


Figure 31: *Visible Image of Southeast USA*

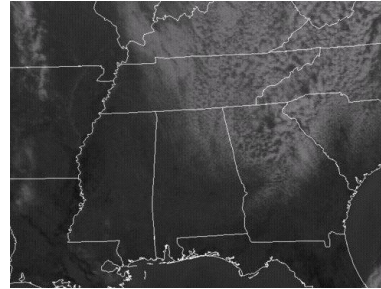


Figure 32: *Infrared Image of Southeast USA*

Ref: www.theweatherprediction.com

For our attempt to locate water exhalation from ground, the IR detection is the most convenient way of detection, because the amount of water descending from the ground is not enough to be visible to the naked eye. The question resulting is, if the emitted radiation of the water vapor exceeds the detection threshold of the device.

There are some more ways to detect water vapor, for example the use of silicon oxide or an gravimetric hygrometer.

Absorptionshygrometer: includes a hygroscopic (water affine) material which changes its properties when getting in contact with vapor. Best known is the hair hygrometer works with a human hair which changes length when comes in contact with moisture. It is an approximate length difference of 2.5% at 0% to 100% humidity.

Psychrometer: which consists of two identical Thermometers, one of them is warped into a moistured mull stocking. The "wet" Thermometer shows a lower temperature then the other, with this information it is possible to calculate the actual humidity.

Dew point mirror hygrometer: This technique of measurement is used to define the national humidity standards. A mirror is cooled until the humidity will settle out, using a light source and a photo receptor the moment of condensation will be determined. The dew point is defined by dew point-temperature and pressure, therefore it is possible to directly calculate the relative humidity.

The problem with these methods is that they are just measuring one single point nearby the instrument or that the accuracy is limited. So, a solution is needed to detect water vapor descending from earth in a designated area.

3.2.1 How to detect water vapor near ground

Reference: [22, Wikipedia (en), 2012]

One possible option would be to use an infrared device which is capable to detect the difference in temperature in a defined area, so it is possible to detect water vapor indirectly over the change of temperature in different areas. So one obtains a vector to walk to for a new measurement. The biggest advance in this method is, that the technology is already in use and easy to apply on this new task.

The other possible method is more of an theoretical approach on how water could be detected underneath the earth. In this method, the infrasound produced by the underground water flow is the signal to be measured. This task would be performed with special microphones, capable to detect frequencies from 0.001 Hz to 20Hz. The greatest issue is that there needs to be a water current to provide the source for the infra sound. Right now infrasound monitoring stations are used to detect earthquakes and possible nuclear detonations (see Figure 33).



Figure 33: *Infrasound arrays at infrasound monitoring station in Qaanaaq, Greenland.*

Ref: *The Official CTBTO Photostream, http://en.wikipedia.org/wiki/File:Infrasound_Arrays.jpg*

4 Resume

For the approach to use the polarized skylight for navigation, it is possible to realize this project using the defined MEMS installed in a sunglass like device and to be autonomous of energy sources, it could be connected to an accumulator, energized by a solar panel.

For the possibility to detect descending water vapor from earth, it is more difficult to realize. The exact detection is rarely impossible to visualize. The most appropriate way would be to detect water indirectly over the temperature variations near ground.

Another way to detect water flow underneath the earth can be realized via the descending infrasound from the current.

References

- [1] [http://en.wiktionary.org/wiki/not_in_Kansas_anymore] *The Wizard of Oz*, visited 7th June 2012, 09:50 CET
- [2] [Bence Suhai and Gábor Horváth] *well does the Rayleigh model describe the E-vector distribution of skylight in clear and cloudy conditions? A full-sky polarimetric study*, OSA A, Vol. 21, Issue 9, pp. 1669-1676 (2004)
- [3] [<http://de.wikipedia.org/wiki/Haidinger-B%C3%BCschel>] *Wilhelm Ritter von Haidinger*, visited 31th October 2012, 20:47 CET
- [4] [T. Labhart and E. P. Meyer] *Detectors for Polarized Skylight in Insects: A Survey of Ommatidial Specializations in the Dorsal Rim Area of the Compound Eye*, in: *Microscopy Research and Technique*, Vol. 47, pp 368–379, 1999
- [5] [T. Labhart et al] *The physiology of the cricket's compound eye with particular reference to the anatomically specialized dorsal rim area*, in: *Journal of Comparative Physiology A*, Vol. 155, pp 289-296, 1984
- [6] [M. L. Brines and J. L. Gould] *Skylight polarisation patterns and animal orientation*, in: *Journal of Experimental Biology*, Vol. 96, pp 69–91, 1982
- [7] [F. G. Valera and W. Witanen] *The Optics of the Compound Eye of the honeybee (Apis mellifera)*, in: *The Journal of General Physiology*, Vol. 55, pp 336–358, 1970
- [8] [http://en.wikipedia.org/wiki/Rayleigh_sky_model] *Rayleigh sky model*, last visited on 1st September 2011, 17:15
- [9] [<http://de.wikipedia.org/wiki/Haidinger-Büschel>] *Haidinger-Büschel*, last visited on 1st October 2011, 19:25
- [10] [Leif K. Karlsen] *Viking Navigation Using the sunstone, Polarized light and the Horizon board*, in: *Navigation Notes*, Issue 93, pp 5-8, <http://www.nordskip.com/navnotes.pdf>, last visited 7th June 2012, 09:54 CET
- [11] [S. Rossel and R. Wehner] *The bee's map of the e-vector pattern in the sky*, in: *Proceedings of the National Academy of Sciences USA*, Vol. 79, pp 4451–4455, 1982
- [12] [Wehner R.] *The Biology of Photoreceptors*, Symposia of the Society for Experimental Biology, Eds. Consens, D. & Vince-Prue, D. Cambridge Univ. Press, London, 1982
- [13] [A. Horridge] *Commentary What does an insect see?*, in: *The Journal of Experimental Biology*, Vol. 212, pp 2721–2729, 2009
- [14] [S. Heinze and U. Homberg] *Maplike Representation of Celestial E-Vector Orientation in the Brain of an Insect*, in: *Science*, Vol. 315, pp. 995, 2007
- [15] [A.M. Scott and A.C. Lewin and K.D. Ridley] *United States Patent Application Publication*, in: *US Patent Application*, Pub.No.: US 2008/0266553A1, 30th October 2008
- [16] [<http://de.wikipedia.org/wiki/Sonnenstrahlung>] *Sonnenstrahlung*, last visited 30th October 2012, 22:01 CET
- [17] [http://en.wikipedia.org/wiki/Rayleigh_sky_model] *Rayleigh sky model*, last visited, 7th June 2012, 09:58 CET

- [18] [<http://de.wikipedia.org/wiki/Wasserdampf>] *Wasserdampf/Water Vapor*, last visited 31th October 2012, 11:45 CET
- [19] [M.H. Schertenleib and H. Egli-Bronz] *Globale Klimatologie: Meteorologie, Wetterinformation und Klimatologie*, 1st Issue, ISBN: 978-3-7155-9123-0, pp 13–14 and 57–62, 2003
- [20] [W.B. Rossow and L. C. Garder] *Cloud Detection Using Satelite Measurements of Infrared and Visible Radiances for ISCCP*, Journal of Climate, Vol. 6, pp 2341–2369, 1993
- [21] [<http://www.theweatherprediction.com/habyhints2/512/>] *Cloud Detection by Meteorologist Jeff Haby*, last visited 31th October 2012, 11:45 CET
- [22] [<http://en.wikipedia.org/wiki/Infrasound>] *Infrasound*, last visited 31th October 2012, 12:09 CET

List of Figures

1	Ref: Halsw, http://en.wikipedia.org/wiki/File:Degpolred.jpg , last visited 7 th June 2012, 10:00 CET	2
2	Ref: Mydriatic, vectorised by chris, http://de.wikipedia.org/w/index.php?title=Datei:Azimuth-Simple.svg&filetimestamp=20090725154905 , last visited 7 th June 2012, 10:03 CET	3
3	Ref: Halsw, http://en.wikipedia.org/w/index.php?title=File:Rayleigh-geometry.pdf&page=1 , last visited 7 th June 2012, 10:03 CET	3
4	Ref: Halsw, http://en.wikipedia.org/wiki/File:Soldis_zendis.jpg , last visited 7 th June 2012, 10:04 CET	4
5	Ref: Halsw, http://en.wikipedia.org/wiki/File:Solang_ztelan_stelan.jpg , last visited 7 th June 2012, 10:04 CET	4
6	Ref: Milvus Passer, http://de.wikipedia.org/w/index.php?title=Datei:Haidinger.klein.jpg&filetimestamp=20090319235851 , last visited 7 th June 2012, 10:07 CET	5
7	Ref: Mivlus Passer, http://de.wikipedia.org/w/index.php?title=Datei:Explanation.Haidinger.jpg&filetimestamp=20090618153508 , last visited 7 th June 2012, 10:08 CET	5
8	Ref: Leif K. Karlsen, <i>Viking Navigation Using the sunstone, Polarized light and the Horizon board</i> , in: Navigation Notes, Issue 93, pp 5-8, http://www.nordskip.com/navnotes.pdf , last visited 7 th June 2012, 10:00 CET	6
9	Ref: Leif K. Karlsen, <i>Viking Navigation Using the sunstone, Polarized light and the Horizon board</i> , in: Navigation Notes, Issue 93, pp 5-8, http://www.nordskip.com/navnotes.pdf , last visited 7 th June 2012, 10:00 CET	7
10	Ref: en.wikipedia.org, http://en.wikipedia.org/wiki/Compound_eye#Compound_eyes , last visited 7 th June 2012, 10:15 CET	8
11	Ref: Penzlin H.: <i>Lehrbuch der Tierphysiologie</i> , Vers. 7, München: Spektrum Akademischer Verlag, 2005, pp 781–784	8
12	Ref: T. Lambhart and E.P. Meyer, <i>Detectors for Polarized Skylight in Insects: A Survey of Ommatidial Specializations in the Dorsal Rim Area of the Compound Eye</i> , in: Microscopy Research and Technique, Vol. 47, p 372, 1999	9
13	Ref: T. Lambhart and E.P. Meyer, <i>Detectors for Polarized Skylight in Insects: A Survey of Ommatidial Specializations in the Dorsal Rim Area of the Compound Eye</i> , in: Microscopy Research and Technique, Vol. 47, p 372, 1999	9
14	Ref: L. Howard and K. Connolly, http://en.wikipedia.org/wiki/File:Human_jejenum_microvilli_2_-_TEM.jpg , last visited 7 th June 2012, 10:19 CET	10
15	Ref: Great Soviet Encyclopedia, http://en.wikipedia.org/wiki/File:Compound_eye1.jpg , last visited 7 th June 2012, 10:20 CET	11
16	Ref: B. Schricker and B. Polaczek, <i>Seminar: Biologie der Bienen</i> , Author: Marco Block	11
17	Ref: T. Lambhart and E.P. Meyer, <i>Detectors for Polarized Skylight in Insects: A Survey of Ommatidial Specializations in the Dorsal Rim Area of the Compound Eye</i> , in: Microscopy Research and Technique, Vol. 47, p 372, 1999	13
18	Ref: A.M. Scott and A.C. Lewin and K.D. Ridley <i>United States Patent Application Publication</i> , in: US Patent Application, Pub.No.: US 2008/0266553A1, 30. Oct.2008	14
19	Ref: A.M. Scott and A.C. Lewin and K.D. Ridley, <i>United States Patent Application Publication</i> , in: US Patent Application, Pub.No.: US 2008/0266553A1, 30. Oct.2008	15
20	Ref: Photograph and Copyright by Iwan Ramawan. Permission to use his Photo within this Paper is approved. http://500px.com/photo/3277004 , last visited 7 th June 2012 10:35 CET	16

21	Ref: Werner Rose. Original uploader Bupresits at de.wikipedia, http://de.wikipedia.org/w/index.php?title=Datei:Acrocinus_longimanus.jpg&filetimestamp=20101024111847 , last visited 7 th June 2012 10:43 CET	16
22	Ref: University Lund, http://www.g-o.de/wissen-aktuell-1356-2004-08-11.html , last visited 7 th June 2012, 12:30 CET	17
23	Ref: Degreen at de.wikipedia, later Quilbert at de.wikipedia, http://de.wikipedia.org/w/index.php?title=Datei:Sonne_Strahlungsintensitaet.svg&filetimestamp=20100509202305 , last visited 7 th June 2012, 10:48 CET	17
24	Ref: NASA Earth Observatory, http://earthobservatory.nasa.gov/IOTD/view.php?id=44267 , last visited 5 th June 2012, 09:40 CET	18
25	Ref: Cepheiden, http://de.wikipedia.org/w/index.php?title=Datei:Oblique_rays_04_Pengo_DE.svg&filetimestamp=20110223080939 , last visited 5 th June 2012, 14:14 CET	19
26	Ref: Hukseflux2008, http://de.wikipedia.org/w/index.php?title=Datei:Pyranometer_sr11_hukseflux.gif&filetimestamp=20080805101001 , last visited 5 th June 2012, 21:01 CET	19
27	Ref: Saperaud, http://de.wikipedia.org/w/index.php?title=Datei:Atmospheric_Water_Vapor_Mean.2005.030.jpg&filetimestamp=20050730141431 , last visited 7 th June 2012, 10:52 CET	20
28	Ref: Markus Schweiß, http://de.wikipedia.org/w/index.php?title=Datei:TS-Wasserdampf_100.png&filetimestamp=20051217215345 , last visited 7 th June 2012, 10:54 CET	21
29	Ref: Markus Schweiß, http://de.wikipedia.org/w/index.php?title=Datei:HS-Wasserdampf_SW.png&filetimestamp=20051207070514 , last visited 7 th June 2012, 10:55 CET	22
30	Ref: Markus Schweiß, http://de.wikipedia.org/w/index.php?title=Datei:Feuchte_Luft.png&filetimestamp=20051120170646 , last visited 7 th June 2012, 10:56 CET	23
31	Ref: www.theweatherprediction.com, http://theweatherprediction.com/habyhints2/512/ , last visited 7 th June 2012, 10:57 CET	24
32	Ref: www.theweatherprediction.com, http://theweatherprediction.com/habyhints2/512/ , last visited 7 th June 2012, 10:57 CET	24
33	Ref: The Official CTBTO Photostream, http://en.wikipedia.org/wiki/File:Infra-sound_Arrays.jpg , last visited 7 th June 2012, 11:00 CET	25
34	Oliver Futterknecht, Malaysia, Kuala Lumpur, 17 th September 2011	30
35	Oliver Futterknecht, Malaysia, Kuala Lumpur, 17 th September 2011	30
36	Oliver Futterknecht, Malaysia, Kuala Lumpur, 17 th September 2011	30
37	Oliver Futterknecht, Malaysia, Kuala Lumpur, 17 th September 2011	30
38	Oliver Futterknecht, Malaysia, Kuala Lumpur, 17 th September 2011	30
39	Oliver Futterknecht, Malaysia, Kuala Lumpur, 17 th September 2011	30
40	Oliver Futterknecht, Malaysia, Kuala Lumpur, 17 th September 2011	31
41	Oliver Futterknecht, Malaysia, Kuala Lumpur, 17 th September 2011	31
42	Oliver Futterknecht, Malaysia, Kuala Lumpur, 17 th September 2011	31
43	Oliver Futterknecht, Malaysia, Kuala Lumpur, 17 th September 2011	31
44	Oliver Futterknecht, Malaysia, Kuala Lumpur, 17 th September 2011	31
45	Oliver Futterknecht, Malaysia, Kuala Lumpur, 17 th September 2011	31
46	Oliver Futterknecht, Malaysia, Kuala Lumpur, 17 th September 2011	32
47	Oliver Futterknecht, Malaysia, Kuala Lumpur, 17 th September 2011	32
48	Oliver Futterknecht, Malaysia, Kuala Lumpur, 17 th September 2011	32
49	Oliver Futterknecht, Malaysia, Kuala Lumpur, 17 th September 2011	32

5 Appendix

The images below show the varying colors throughout the day (i.e., with changing skylight polarization) of a Corderite stone. Such color change might have helped the Vikings in their navigation [10, (Leif K. Karlsen, www.nordskip.com/navnotes.pdf)].



Figure 34: *Corderit crystal, Kuala Lumpur, Malaysia, 17th Sept., 2011, 02:43pm*



Figure 35: *Corderit crystal, Kuala Lumpur, Malaysia, 17th Sept., 2011, 03:00pm*



Figure 36: *Corderit crystal, Kuala Lumpur, Malaysia, 17th Sept., 2011, 03:14pm*



Figure 37: *Corderit crystal, Kuala Lumpur, Malaysia, 17th Sept., 2011, 03:31pm*



Figure 38: *Corderit crystal, Kuala Lumpur, Malaysia, 17th Sept., 2011, 03:45pm*



Figure 39: *Corderit crystal, Kuala Lumpur, Malaysia, 17th Sept., 2011, 04:00pm*



Figure 40: *Corderit crystal, Kuala Lumpur, Malaysia, 17th Sept., 2011, 04:16pm*



Figure 41: *Corderit crystal, Kuala Lumpur, Malaysia, 17th Sept., 2011, 04:32pm*



Figure 42: *Corderit crystal, Kuala Lumpur, Malaysia, 17th Sept., 2011, 04:50pm*



Figure 43: *Corderit crystal, Kuala Lumpur, Malaysia, 17th Sept., 2011, 05:06pm*



Figure 44: *Corderit crystal, Kuala Lumpur, Malaysia, 17th Sept., 2011, 05:21pm*



Figure 45: *Corderit crystal, Kuala Lumpur, Malaysia, 17th Sept., 2011, 05:36pm*



Figure 46: *Corderit crystal, Kuala Lumpur, Malaysia, 17th Sept., 2011, 05:53pm*



Figure 47: *Corderit crystal, Kuala Lumpur, Malaysia, 17th Sept., 2011, 06:10pm*



Figure 48: *Corderit crystal, Kuala Lumpur, Malaysia, 17th Sept., 2011, 06:26pm*



Figure 49: *Corderit crystal, Kuala Lumpur, Malaysia, 17th Sept., 2011, 07:00pm*

It can be easily seen, that with the descending of the sun the yellowish shine descends from the middle to the bottom of the crystal and vanishes around 6:00pm. Important to say that during this experiment, the sun wasn't always directly visible and there was also a rainshower. Even with this changing weather conditions, there can be seen a constant changing in colors during the sun descending as showed in the following table:

Figure	R	G	Hex-Code	Sample
34	141	122	#8D7A92	
35	150	129	#968198	
36	164	122	#A47A88	
37	134	126	#867E99	
38	127	114	#7F7289	
39	122	115	#7A738E	
40	123	113	#7B7180	
41	147	121	#937984	
42	147	121	#8E7E00	
43	141	127	#8D7F00	
44	139	126	#8B7E00	
45	135	115	#877300	
46	131	112	#837000	
47	146	125	#927D00	
48	148	130	#948200	
49	97	79	#614F00	

Table 1: *This table show the amount of Red and Green (measured with Photoshop Elements 9 in an area at the center of the crystal), the Hex-Code and a Sample of the yellow-part of the color mixing. The blue part of the spectrum is not used because it is the basic color of the gemstone and hardly changes. The two peaks of darker areas arose because of the rainshower and the following more intense sunlight which has followed.*